Heterogeneous Catalysis

DOI: 10.1002/ange.201410360

Nanoscale Magnetic Stirring Bars for Heterogeneous Catalysis in Microscopic Systems**

Shuliang Yang, Changyan Cao, Yongbin Sun, Peipei Huang, Fangfang Wei, and Weiguo Song**

Abstract: *Nanometer-sized magnetic stirring bars containing Pd nanoparticles (denoted as Fe_3O_4-NC-PZS-Pd) for heterogeneous catalysis in microscopic system were prepared through a facile two-step process. In the hydrogenation of styrene, Fe_3O_4-NC-PZS-Pd showed an activity similar to that of the commercial Pd/C catalyst, but much better stability. In microscopic catalytic systems, Fe_3O_4-NC-PZS-Pd can effectively stir the reaction solution within microdrops to accelerate mass transfer, and displays far better catalytic activity than the commercial Pd/C for the hydrogenation of methylene blue in an array of microdroplets. These results suggested that the Fe_3O_4-NC-PZS-Pd could be used as nanoscale stirring bars in nanoreactors.*

Effective mixing of reactants is beneficial for mass transport in chemical reactions, especially in heterogeneous catalysis, to enhance the reaction rate and reduce energy consumption.[1] For optimal mixing, magnetic stirring bars or mechanical stirrers are usually used in reactors of various sizes. However, conventional stirring methods cannot be used in nanoscale reactors such as microdroplets or micelles, which are of great importance for lab-on-chip applications[2] and microliter bioassay,[3] because conventional stirring bars are much larger than the nanoscale reactor. Therefore, it is necessary to design nanometer-sized stirring bars that are sufficiently small but still able to rotate under external influence. In this study, we produced such nanoscale magnetic stirring bars.

Magnetic stirring is the most convenient option for stirring. For microscopic systems, the size of the magnetic stirrer must be within nanoscale. Thus, magnetic nanoparticles are usually assembled into rigid nanochains. Previous reports showed that magnetic induction[4] and external coating by induced self-assembly[5] are two effective methods for forming magnetic nanochains with nanoparticles. Some nanometer-sized magnetic stirring bars based on nanochains have been reported. For example, Pyun et al. reported polystyrene-coated cobalt nanoparticles, which were assembled into nanochains with the help of surfactants.[5a] Chen's group prepared a nanometer-sized magnetic stirring bar,[4b] by first assembling Fe_3O_4 nanoparticles to form a 1D chain, which was then preserved in silica shells. The SiO_2 shell endowed the Fe_3O_4 magnetic chains with rigidity and quick response to a common magnetic stirring plate, and the nanostirrer could rotate quickly inside small droplets. However, so far there is no report about the use of nanometer-sized magnetic stirring bars in heterogeneous catalysis.

Herein, we report a facile two-step synthesis method to produce nanometer-sized magnetic stirring bars that contain Pd nanoparticles for heterogeneous catalysis in microscopic systems. The preparation process is illustrated in Scheme 1.

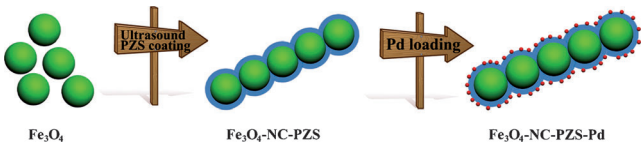

Scheme 1. Preparation of Fe_3O_4-NC-PZS-Pd catalytically active magnetic stirring bars.

Fe_3O_4 nanoparticles were prepared as building blocks for 1D nanochains (denoted as Fe_3O_4-NC).[6] With the help of ultrasound and the paramagnetic response of Fe_3O_4 nanoparticles, a highly cross-linked polymer poly(cyclotriphosphazene-*co*-4,4′-sulfonyldiphenol) (PZS, please see Figure S1 for the polymer structure) was coated as the shell to stabilize the Fe_3O_4 nanochains (denoted as Fe_3O_4-NC-PZS).[7] The PZS coating also provided functional sites to anchor the Pd nanoparticles onto the surface of Fe_3O_4-NC-PZS[8] to produce the catalytically active stirring bars (denoted as Fe_3O_4-NC-PZS-Pd). In tiny microdrops, in which a conventional stirring bar could not be used, the synthesized Fe_3O_4-NC-PZS-Pd could stir the microdrops to accelerate mass transfer, and displayed far better catalytic activity than the commercial Pd/C during the hydrogenation of arrays of microdroplets containing methylene blue (MB).

As shown in Figure 1a, the synthesized Fe_3O_4 nanoparticles exhibited uniform morphology with diameters of about 250 ± 20 nm. Under ultrasonic irradiation, the Fe_3O_4 nanoparticles were assembled into nanochains (Figure 1b), and PZS shells were formed and coated the Fe_3O_4 nanochains through in situ polymerization.[7,9] As shown in Figure 1c, the amorphous polymer layer was quite even and thin (red dashed line in Figure 1c). The presence of nitrogen atoms in the PZS coating could act as anchor sites to stabilize Pd nanoparticles due to the strong affinity of N for Pd.[10] Based on this design, Pd nanoparticles were loaded onto the surface

[*] S. Yang, Dr. C. Cao, Y. Sun, P. Huang, F. Wei, Prof. W. Song
Beijing National Laboratory for Molecular Sciences
Laboratory of Molecular Nanostructures and Nanotechnology
Institute of Chemistry, Chinese Academy of Sciences
100190, Beijing (China)
E-mail: cycao@iccas.ac.cn
wsong@iccas.ac.cn

[**] We thank the National Basic Research Program of China (2011CB933700), the National Natural Science Foundation of China (NSFC 21333009, 21273244), and the Chinese Academy of Sciences (KJCX2-YW-N41) for financial support.

Supporting information for this article is available on the WWW under http://dx.doi.org/10.1002/anie.201410360.

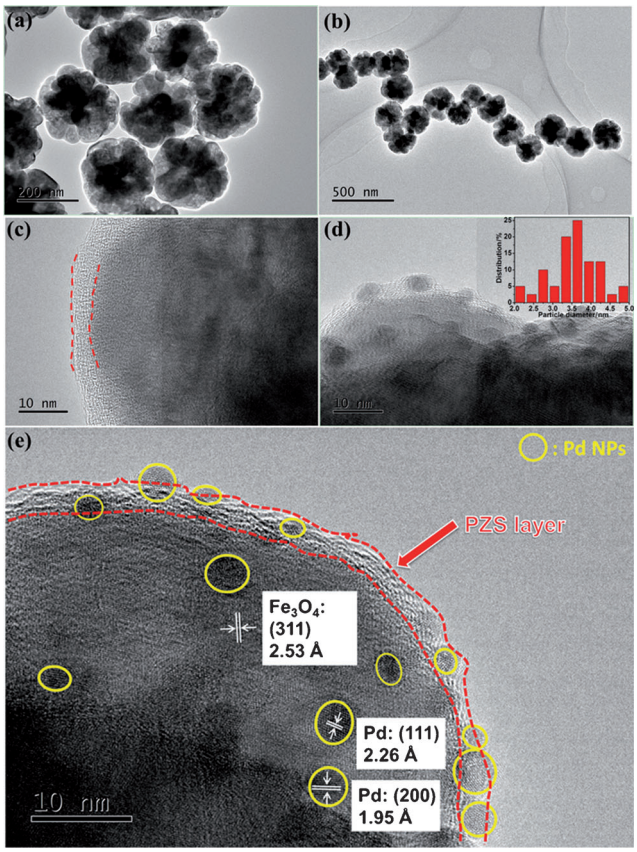

Figure 1. TEM images of the Fe_3O_4 nanocrystal clusters (a) and Fe_3O_4 nanochains with PZS coating (b, c) and the Fe_3O_4-NC-PZS-Pd (d, e). Inset of Figure 1 d: Distribution of Pd nanoparticles in Fe_3O_4-NC-PZS-Pd.

of Fe_3O_4-NC-PZS.[8] After Pd loading, the morphology of Fe_3O_4-NC-PZS was maintained. The distribution of Pd nanoparticles was shown in the inset of Figure 1 d. The average diameter of Pd nanoparticles was 3.5 ± 1.5 nm. When the edge of the Fe_3O_4-NC-PZS-Pd was magnified, Pd nanoparticles could be observed (Figure 1 d). PZS layer and lattice fringes of Pd and Fe_3O_4 can be seen in the high-resolution TEM image (Figures 1 e and S2).

Figure S3 shows the XRD pattern of Fe_3O_4-NC-PZS-Pd. Besides the characteristic peaks of Fe_3O_4, relatively weak and broad peaks of Pd could also be observed. Due to the amorphous nature of the PZS layer, no diffraction peak from the PZS layer was observed. The results from XPS analysis confirmed that Fe_3O_4-NC-PZS-Pd contained Fe, Pd, C, O, N, P, Cl, and S (Figure S4). High-resolution XPS of the Pd 3d peak indicated that most of the palladium was metallic Pd (inset of Figure S4a). Comparison of the Pd 3d peak of Fe_3O_4-NC-PZS-Pd with the peak of metallic Pd, showed that the binding energy of Fe_3O_4-NC-PZS-Pd shifted to a lower position, indicating that the N atoms of PZS coordinate with Pd to stabilize it (Figures S4b and S5). Elemental mapping of Fe_3O_4-NC-PZS-Pd also showed that the stirring bars were composed of the desired segments and Pd nanoparticles were distributed uniformly (Figure S6).

Ultrasonic irradiation played a vital role during the PZS coating. In a control experiment, in which only magnetic stirring and no ultrasonic irradiation was employed, the PZS could not be coated uniformly on the surface of Fe_3O_4 nanochains (the sample was denoted as SP-2). Instead, the polymer aggregated by itself, thereby forming irregular particles, and the Pd nanoparticles were located on the surface of PZS but not on the surface of Fe_3O_4 (Figure S7). In another experiment, in which no PZS coating was employed, the Pd nanoparticles tended to aggregate and could not be loaded onto the surface of Fe_3O_4 uniformly (denoted as SP-3, Figure S8).

Due to the presence of Fe_3O_4 nanochains, the prepared Fe_3O_4-NC-PZS-Pd stirring bars displayed good magnetic response. They could be used as stirrer as well as catalyst in the solution (see Video S1 in the Supporting Information, SI). The hydrogenation of styrene was chosen as a model reaction to test the heterogeneous catalysis properties of Fe_3O_4-NC-PZS-Pd.[11] No commercial magnetic stirring bar was used. Compared to the other two samples (SP-2, SP-3), Fe_3O_4-NC-PZS-Pd exhibited the best catalytic activity (Figure S9). We ascribed this result to the following two reasons: one is the better dispersivity of Pd nanoparticles on Fe_3O_4-NC-PZS-Pd; the other is the better mixing effects due to the Fe_3O_4 nanochains in the Fe_3O_4-NC-PZS-Pd.

The catalytic activity of Fe_3O_4-NC-PZS-Pd was comparable to that of commercial Pd/C at the same weight percent of Pd (Figure 2 a). However, Fe_3O_4-NC-PZS-Pd showed much

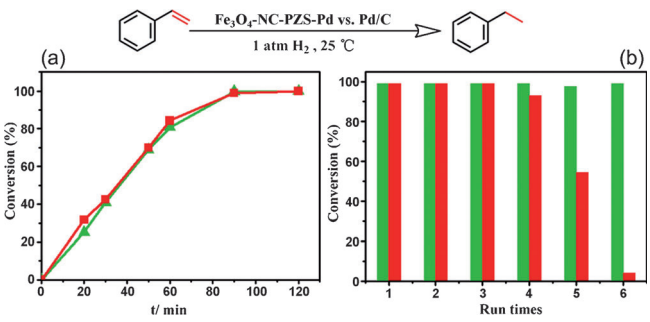

Figure 2. a) Conversion versus reaction time curve for styrene hydrogenation with Fe_3O_4-NC-PZS-Pd (green curves) and Pd/C (red curves) as catalysts, respectively. b) Recycling of Fe_3O_4-NC-PZS-Pd (green columns) and commercial Pd/C (red columns) catalyst using styrene hydrogenation as model reaction.

better stability during cycling tests. There was no obvious decrease of activity after six cycles. In contrast, an obvious activity decrease was observed for the commercial Pd/C after three runs (Figure 2 b). After the reaction, the supernatant of the Fe_3O_4-NC-PZS-Pd reaction system was analyzed by inductively coupled plasma atom emission spectroscopy (ICP-AES), and no Pd was detected. TEM images showed that after multiple catalytic cycles, Fe_3O_4-NC-PZS-Pd maintained its morphology and the Pd nanoparticles were still loaded on the surface of the PZS layer (Figure S10). Substrate expansion and TOF values are presented in Table S1. The results showed the excellent catalytic activity of Fe_3O_4-NC-PZS-Pd for different substrates.

Such an excellent stability could be ascribed to the following reasons: 1) the N atoms in the PZS act as anchor

sites to immobilize Pd nanoparticles, which efficiently prevents the aggregation and leaching of Pd nanoparticle. 2) The PZS layer protects the Fe_3O_4 internal core from the corrosion. This protection is advantageous for the integrity of the catalyst. 3) When the reaction was finished, Fe_3O_4-NC-PZS-Pd can be attracted by an external magnet and recovered easily with essentially no loss. However, the Pd/C catalyst was still dispersed in solution (Figure S11) and has to be recovered by centrifugation. The facile recovery is beneficial for recycling of the catalyst and decreases the catalyst loss.

During a strong-acid corrosion test, the Fe_3O_4 internal core of Fe_3O_4-NC-PZS-Pd was maintained after 48 h in concentrated nitric acid, whereas the SP-3 sample, which has no PZS protection layer, was completely dissolved (Figure S12). This test confirmed that due to the protection of the PZS layer Fe_3O_4-NC-PZS-Pd can be used in corrosive solutions.

In microscopic catalytic systems, commercial magnetic stirring bars cannot be used.[12] We envisioned that Fe_3O_4-NC-PZS-Pd might be especially useful in microscopic system, in which the mixing of reactants must be achieved by nanostirrers. To test the catalytic activity of Fe_3O_4-NC-PZS-Pd in a microscopic system, the hydrogenation of methylene blue (MB) in arrays of microdroplets was chosen as a model reaction (the color change of the blue MB solution is a direct indicator of the reaction progress).[13] As shown in Figure 3,

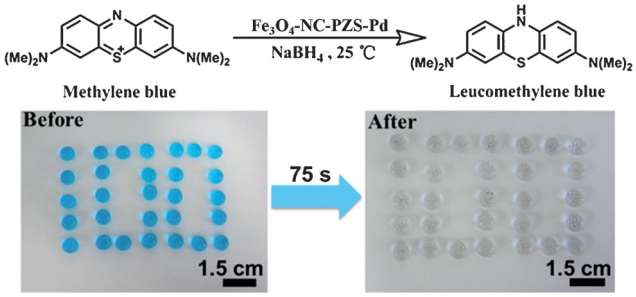

Figure 3. Hydrogenation of methylene blue (MB) in arrays of microdroplets with Fe_3O_4-NC-PZS-Pd as magnetic stirring bars and catalyst.

the blue microdroplets became colorless in 75 s after adding Fe_3O_4-NC-PZS-Pd. In Video S2 (SI), the rotation of Fe_3O_4-NC-PZS-Pd during the reaction process can be observed when the magnetic stirring plate was turned on. In comparison, the reaction rate with Pd/C as catalyst was much lower than that of Fe_3O_4-NC-PZS-Pd (video S3).This was due to the far better mixing in the microscopic system containing Fe_3O_4-NC-PZS-Pd. This assumption was confirmed by the result that the fading of MB became slower when the magnetic stirrer was turned off, even though the same amount of Fe_3O_4-NC-PZS-Pd was added.

These nanoscale magnetic stirring bars are not limited to Pd. Pt nanoparticles could also be loaded onto the PZS layer (Figure S13).[14] From the TEM images, Pt nanoparticles with an average diameter of ca. 3 nm were also successfully loaded onto the surface of Fe_3O_4 nanochains. Both the XRD pattern and high-resolution XPS analysis confirmed that Pt nanoparticles existed as zero-valent.

In summary, we produced nanoscale catalytically active magnetic stirring bars for microscopic catalytic system. In the hydrogenation of styrene, the Fe_3O_4-NC-PZS-Pd catalyst showed catalytic activity comparable to that of the commercial Pd/C catalyst and far better stability. When the hydrogenation of MB was run in microdroplets, in which conventional stirring bars cannot be used, the Fe_3O_4-NC-PZS-Pd catalyst showed remarkable ability to mix the reactants inside small liquid droplets and achieved superior catalytic activity.

Received: October 22, 2014
Published online: January 21, 2015

Keywords: heterogeneous catalysis · magnetic stirring bars · microscopic systems · nanoparticles

[1] a) J. M. Ottino, *Science* **2004**, *305*, 485 – 486; b) J. E. Martin, K. J. Solis, *Soft Matter* **2014**, *10*, 3993 – 4002; c) A. J. deMello, *Nature* **2006**, *442*, 394 – 402; d) Z. C. Wang, W. Chen, Z. L. Han, J. Zhu, N. Lu, Y. Yang, D. K. Ma, Y. Chen, S. M. Huang, *Nano Res.* **2014**, *7*, 1254 – 1262; e) Ö. Metin, S. F. Ho, C. Alp, H. Can, M. N. Mankin, M. S. Gültekin, M. F. Chi, S. H. Sun, *Nano Res.* **2013**, *6*, 10 – 18.

[2] a) S. Haeberle, R. Zengerle, *Lab Chip* **2007**, *7*, 1094 – 1110; b) L. D. Mao, H. Koser, *Nanotechnology* **2006**, *17*, S34 – S47; c) A. van Reenen, A. M. de Jong, J. M. J. den Toonder, M. W. J. Prins, *Lab Chip* **2014**, *14*, 1966 – 1986.

[3] a) X. Mao, B. K. Juluri, M. I. Lapsley, Z. S. Stratton, T. J. Huang, *Microfluid. Nanofluid.* **2010**, *8*, 139 – 144; b) H.-B. Lee, K. Oh, W.-H. Yeo, T.-R. Lee, Y.-S. Chang, J.-B. Choi, K.-H. Lee, J. Kramlich, J. J. Riley, Y.-J. Kim, J.-H. Chung, *Microfluid. Nanofluid.* **2012**, *12*, 143 – 156.

[4] a) G. Cheng, D. Romero, G. T. Fraser, A. R. Hight Walker, *Langmuir* **2005**, *21*, 12055 – 12059; b) W. H. Chong, L. K. Chin, R. L. S. Tan, H. Wang, A. Q. Liu, H. Chen, *Angew. Chem. Int. Ed.* **2013**, *52*, 8570 – 8573; *Angew. Chem.* **2013**, *125*, 8732 – 8735; c) P. Y. Keng, B. Y. Kim, I.-B. Shim, R. Sahoo, P. E. Veneman, N. R. Armstrong, H. Yoo, J. E. Pemberton, M. M. Bull, J. J. Griebel, E. L. Ratcliff, K. G. Nebesny, J. Pyun, *ACS Nano* **2009**, *3*, 3143 – 3157; d) Y. Nagaoka, H. Morimoto, T. Maekawa, *Langmuir* **2011**, *27*, 9160 – 9164.

[5] a) B. D. Korth, P. Keng, I. Shim, S. E. Bowles, C. Tang, T. Kowalewski, K. W. Nebesny, J. Pyun, *J. Am. Chem. Soc.* **2006**, *128*, 6562 – 6563; b) K. Nakata, Y. Hu, O. Uzun, O. Bakr, F. Stellacci, *Adv. Mater.* **2008**, *20*, 4294 – 4299; c) J. Townsend, R. Burtovyy, Y. Galabura, I. Luzinov, *ACS Nano* **2014**, *8*, 6970 – 6978.

[6] H. Deng, X. Li, Q. Peng, X. Wang, J. Chen, Y. Li, *Angew. Chem. Int. Ed.* **2005**, *44*, 2782 – 2785; *Angew. Chem.* **2005**, *117*, 2842 – 2845.

[7] J. Zhou, L. Meng, X. Feng, X. Zhang, Q. Lu, *Angew. Chem. Int. Ed.* **2010**, *49*, 8476 – 8479; *Angew. Chem.* **2010**, *122*, 8654 – 8657.

[8] a) Z. Chen, Z.-M. Cui, P. Li, C.-Y. Cao, Y.-L. Hong, Z.-Y. Wu, W.-G. Song, *J. Phys. Chem. C* **2012**, *116*, 14986 – 14991; b) Z. Chen, Z.-M. Cui, F. Niu, L. Jiang, W.-G. Song, *Chem. Commun.* **2010**, *46*, 6524 – 6526.

[9] a) J. Fu, X. Huang, Y. Huang, J. Zhang, X. Tang, *Chem. Commun.* **2009**, 1049 – 1051; b) L. Zhu, Y. Xu, W. Yuan, J. Xi, X. Huang, X. Tang, S. Zheng, *Adv. Mater.* **2006**, *18*, 2997 – 3000.

[10] a) A. Fihri, D. Cha, M. Bouhrara, N. Almana, V. Polshettiwar, *ChemSusChem* **2012**, *5*, 85 – 89; b) Z. Li, J. Liu, C. Xia, F. Li, *ACS Catal.* **2013**, *3*, 2440 – 2448; c) K. Zhang, C. H. Chen, X. Zhou, Y. Gong, G. Zhang, X. Wang, Y. Chen, J. Shi, *J. Mater. Chem. A* **2014**, *2*, 1515 – 1523; d) A. Leyva-Pérez, J. Oliver-Meseguer, P.

Rubio-Marqués, A. Corma, *Angew. Chem. Int. Ed.* **2013**, *52*, 11554 – 11559; *Angew. Chem.* **2013**, *125*, 11768 – 11773; e) X. Xu, Y. Li, Y. Gong, P. Zhang, H. Li, Y. Wang, *J. Am. Chem. Soc.* **2012**, *134*, 16987 – 16990; f) P. Zhang, J. Yuan, T.-P. Fellinger, M. Antonietti, H. Li, Y. Wang, *Angew. Chem. Int. Ed.* **2013**, *52*, 6028 – 6032; *Angew. Chem.* **2013**, *125*, 6144 – 6148; g) J. Jia, R. Wang, H. Wang, S. Ji, J. Key, V. Linkov, K. Shi, Z. Lei, *Catal. Commun.* **2011**, *16*, 60 – 63.

[11] a) L. Peng, J. Zhang, J. Li, B. Han, Z. Xue, G. Yang, *Angew. Chem. Int. Ed.* **2013**, *52*, 1792 – 1795; *Angew. Chem.* **2013**, *125*, 1836 – 1839; b) X. Huang, Y. Li, Y. Chen, E. Zhou, Y. Xu, H. Zhou, X. Duan, Y. Huang, *Angew. Chem. Int. Ed.* **2013**, *52*, 2520 – 2524; *Angew. Chem.* **2013**, *125*, 2580 – 2584; c) H. Yang, T. Zhou, W. Zhang, *Angew. Chem. Int. Ed.* **2013**, *52*, 7455 – 7459; *Angew. Chem.* **2013**, *125*, 7603 – 7607.

[12] a) S. L. Biswal, A. P. Gast, *Anal. Chem.* **2004**, *76*, 6448 – 6455; b) I. Petousis, E. Homburg, R. Derks, A. Dietzel, *Lab Chip* **2007**, *7*, 1746; c) T. Roy, A. Sinha, S. Chakraborty, R. Ganguly, I. K. Puri, *Phys. Fluids* **2009**, *21*, 027101.

[13] a) G. Fu, L. Tao, M. Zhang, Y. Chen, Y. Tang, J. Lin, T. Lu, *Nanoscale* **2013**, *5*, 8007 – 8014; b) S.-L. Yang, C.-Y. Cao, F.-F. Wei, P.-P. Huang, Y.-B. Sun, W.-G. Song, *ChemCatChem* **2014**, *6*, 1868 – 1872; c) A. J. Hallock, E. S. F. Berman, R. N. Zare, *J. Am. Chem. Soc.* **2003**, *125*, 1158 – 1159.

[14] a) D. C. Higgins, D. Meza, Z. Chen, *J. Phys. Chem. C* **2010**, *114*, 21982 – 21988; b) S. Chen, Z. Wei, X. Qi, L. Dong, Y.-G. Guo, L. Wan, Z. Shao, L. Li, *J. Am. Chem. Soc.* **2012**, *134*, 13252 – 13255; c) X.-H. Li, X. Wang, M. Antonietti, *Chem. Sci.* **2012**, *3*, 2170 – 2174.